Solar tower power plant using a particle-heated steam generator: Modeling and parametric study

Michael Krüger, Philipp Bartsch, Harald Pointner, and Stefan Zunft

Citation: AIP Conference Proceedings **1734**, 050025 (2016); doi: 10.1063/1.4949123
View online: http://dx.doi.org/10.1063/1.4949123
View Table of Contents: http://scitation.aip.org/content/aip/proceeding/aipcp/1734?ver=pdfcov
Published by the AIP Publishing

Solar Tower Power Plant Using a Particle-Heated Steam Generator: Modeling and Parametric Study

Michael Krüger[1, a)], Philipp Bartsch[1, b)], Harald Pointner[1, c)], Stefan Zunft[1, d)]

[1]German Aerospace Center (DLR), Institute of Technical Thermodynamics, Pfaffenwaldring 38-40, D-70569 Stuttgart, Germany

[a)]Corresponding author: Michael.Krueger@dlr.de
[b)]Philipp.Bartsch@dlr.de
[c)]Harald.Pointer@dlr.de
[d)]Stefan.Zunft@dlr.de

Abstract. Within the framework of the project HiTExStor II, a system model for the entire power plant consisting of volumetric air receiver, air-sand heat exchanger, sand storage system, steam generator and water-steam cycle was implemented in software "Ebsilon Professional". As a steam generator, the two technologies fluidized bed cooler and moving bed heat exchangers were considered. Physical models for the non-conventional power plant components as air-sand heat exchanger, fluidized bed coolers and moving bed heat exchanger had to be created and implemented in the simulation environment. Using the simulation model for the power plant, the individual components and subassemblies have been designed and the operating parameters were optimized in extensive parametric studies in terms of the essential degrees of freedom. The annual net electricity output for different systems was determined in annual performance calculations at a selected location (Huelva, Spain) using the optimized values for the studied parameters. The solution with moderate regenerative feed water heating has been found the most advantageous. Furthermore, the system with moving bed heat exchanger prevails over the system with fluidized bed cooler due to a 6 % higher net electricity yield.

INTRODUCTION

Due to their high conversion temperature, solar tower systems are particularly promising potential for an achievement of a high solar-to-electric efficiency. A novel concept for this technology is based on the use of solid particles both as a heat transfer and a storage medium. Utilizing the cost-effective heat-storage capabilities, a fluctuating electricity demand can be covered with the help of a dispatchable generation.

In a solar tower system, a large number of mirrors (so-called heliostats) focus the direct sunlight onto the receiver on top of a tower. In the receiver, the concentrated solar radiation is absorbed and heats a primary air loop. A thermally coupled secondary loop uses a flowable particle stream: particles coming from the cold storage tank are heated up in an air-sand heat exchanger (ASHX), and the heated particles are transported to the hot storage tank. For electricity production, hot particles are taken from the hot storage and pass through the steam generator, where superheated steam is generated to drive the power cycle. After passing through the steam generator, the cooled particles are put into the cold storage, see Fig. 1.

The particle-heated steam generator used to discharge the hot particle storage is a novel and central component. Besides ASHX, this device is essential for the function of the particle sub-system. In principle, there are two basic technology options to implement it: as a fluidized bed cooler (FBC) or as a moving bed heat exchanger (MBHX), each with specific merits and disadvantages.

The present work considers the system integration of such a particle-heated steam generator and elaborates the differences of both technology options with respect to solar systems electricity output.

SolarPACES 2015
AIP Conf. Proc. 1734, 050025-1–050025-9; doi: 10.1063/1.4949123
Published by AIP Publishing. 978-0-7354-1386-3/$30.00

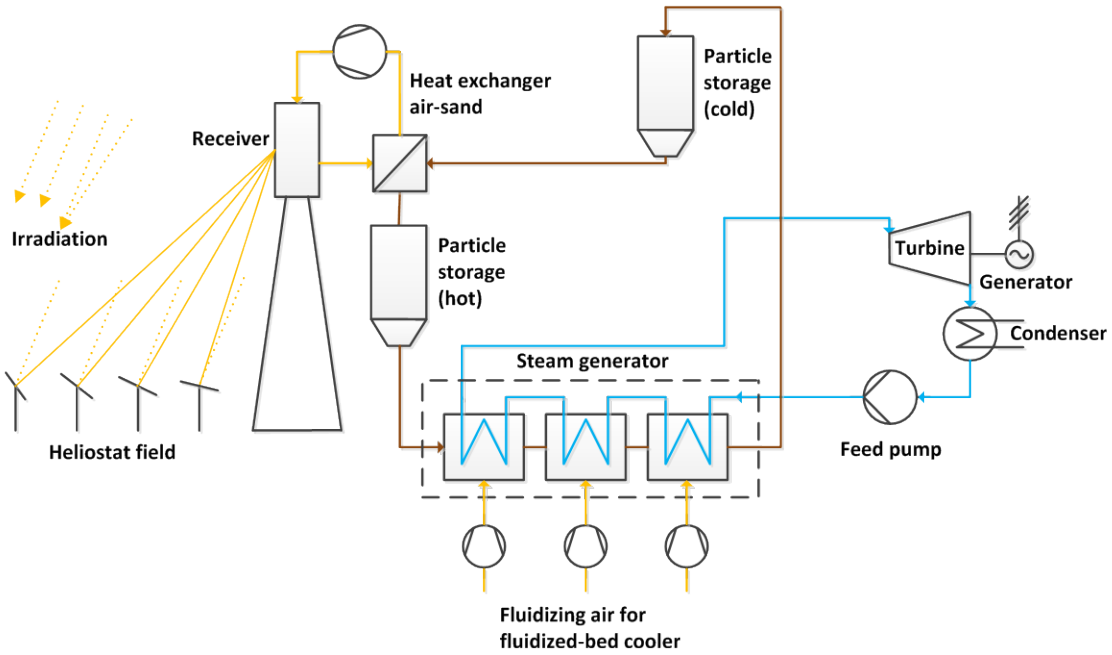

FIGURE 1. Simplified flow diagram of the solar tower power plant cycle using a fluidized bed cooler

SYSTEM MODEL AND MODELING OF THE COMPONENTS

Air Loop

The heliostat field which concentrates the solar energy und focusing on the receiver is not part of the simulation. Therefore the losses that occur within the heliostat field are not considered. A fixed pressure drop ($\Delta p = 0.01$ bar) and efficiency ($\eta = 0.9$) are assumed for the receiver. The air mass flow, passing through the receiver is controlled in order to keep air outlet temperature constant at 850 °C.

Air-Sand Heat Exchanger (ASHX)

The design of the ASHX has great influence on the efficiency of the power plant. The drive power of the fan is proportional to the transported volume flow, and the pressure loss of the cycle. The ASHX has significant influence on both values. On the one hand it represents the component with the highest pressure loss in the air cycle. On the other hand the ASHX affects by a given value of the air outlet temperature the air flow which is required to remove the heat output of the receiver. Therefore it must be find the best compromise between the size and the power requirement of the fan.

Because of its key role already extensive investigations into this apparatus at DLR and the Solar Institute Jülich were carried out in the past [1]. In one of the studied constructions sand moves from the top to the bottom through the apparatus and air flows simultaneously in the cross-flow through the sand bed. Thus, there is direct contact between the two heat transfer media. In order to prevent material discharge in the air loop, the sand is kept between two porous walls. These must be impermeable to the sand and should offer the air a very low resistance at the same time. Furthermore, stringent physical and chemical requirements such as high temperature resistance, abrasion resistance and strength should be fulfilled [2].

The ASHX is modeled as an ideal cross-flow heat exchanger. The heat transfer is calculated by Achenbach [3] and Gnilinski [4]. There, the heat transfer of the bed is calculated by means of empirical factors from the heat transfer at the single particle. The pressure loss in ASHX consists of the pressure drop in the sand bed, which is calculated with the equations given by Wirth in the VDI Heat Atlas [4], and the pressure loss in the two porous walls. To calculate the latter equations for filter from [5] are used. The calculation of a cross-flow heat exchanger is

based on [4]. The transferred heat is the product of heat transfer coefficient, overall surface of the particles present in the apparatus and the mean logarithmic temperature difference between air and sand. The correction factor required for cross-flow heat exchanger in the equation for calculating the average logarithmic temperature difference is calculated according to [6]. The sand mass flow is set so that the desired sand outlet temperature is reached.

Sand Loop

The sand circuit has a storage function, receiving heat from the air loop and giving it to the water-steam cycle. After the hot sand storage sand enters the steam generator. There, the feed water, coming from the condenser is heated to reach the evaporation temperature (economizer), followed by the actual evaporation process in the evaporator and then is the saturated steam to the main steam temperature overheated (superheater). At the same time the sand is cooled to cold sand temperature before leaving the steam generator towards cold sand storage.

The principle of operation of steam generator FBC and MBHX is presented in Fig. 2. They will be described in more detail in the following section.

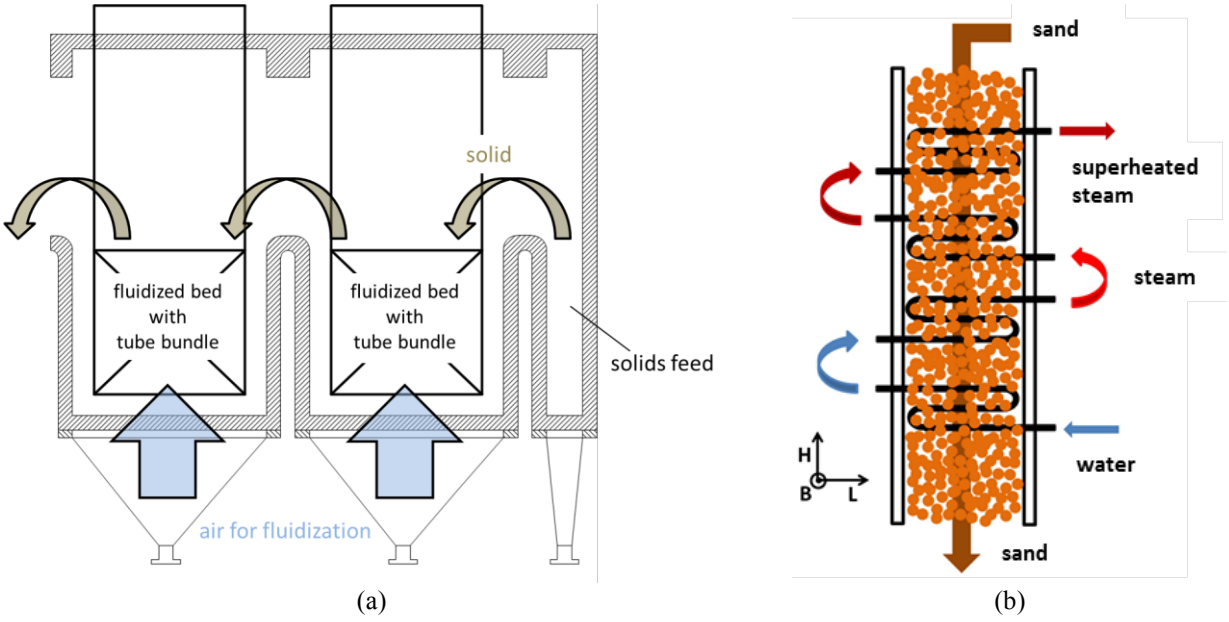

(a) (b)

FIGURE 2. Principle of operation of a fluidized bed cooler (FBC) (a) and a moving bed heat exchanger (MBHX) (b).

Steam Generator

Fluidized Bed Cooler (FBC)

FBC are state of the art [7] and are distributed by various companies such as ThyssenKrupp, Enviro Engineering, Vibra-technology and TEMA Process. The technology is based on principle of the fluidized beds and is characterized by a very good heat and mass transfer [8].

As shown in Fig. 2 (a), the overall system consists of a number of series-connected chambers, which are filled with fluidizable material. The air is blown from below through a nozzle bottom in the chambers, whereby the fluidized material gets "fluidized" and becomes liquid-like. The individual chambers are separated by weirs from each other so that the fluidized material can gradually overflow from one chamber to the next. The fluidized bed temperature decreases continuously from chamber to chamber. The inner space of each chamber is - like in the MBHX – traversed by meandering, aquiferous tube coils. The water passes through the series of fluidized beds in the opposite direction to the sand. Thus, the fluidized beds operate as economizers at colder end, as the evaporator at the middle section and as the superheater on the hot sand inlet side.

The heat transfer within the bulk of bed itself - from the fluid to the solid particles - is generally of minor importance. The heat transfer surface between fluid and surface of all particles is so great that within the layer practically thermal equilibrium exists [9]. Thus it can be assumed that it is a uniform temperature of fluid and particles within the fluidized bed.

The heat transfer within fluidized bed consists of three separate mechanisms, namely gas convection, radiation and particle convection [9]. Gas convection denotes the heat transfer directly from the gas phase to the heat transfer surface at locations that are not occupied by particles [10]. It is calculated here according to Baskakov equation recommended by Schlünder [10]. The heat transfer by radiation is calculated according to Kunii [11]. For the emission coefficients of the fluidized bed a value of 0.86 [11] is assumed. The emission coefficient of the wall is set for oxidized steel with 0.8 [12]. Particle convection denotes the heat exchange when the particles come in contact with the wall. According to Schlünder [10], this mechanism dominates the heat transfer in fluidized beds, whose particles have a diameter of less than about 1 mm. There are many different methods of particle convection heat transfer calculation [11]. In this work, a single particle model is used according to the theory of Martin [9]. Here heat transfer processes of a single particle are considered and then transcribed to the particle collective. The further assumption is that the particles in a fluidized bed behave similar to the molecules in the kinetic theory of gases.

Moving Bed Heat Exchanger (MBHX)

Moving bed heat exchangers are currently still subject of research [13], [14]. Here the sand moves through this apparatus similar to the ASHX from top to bottom (moving bed), see Fig. 2 (b). The moving bed is crossed by water vapor containing horizontal pipes, which are connected to each other by 180° pipe bends. While the sand passes the pipe coils, it transfers its heat to the pipe surface. The steam passes through the moving bed in the meandering pipe coils from bottom to the top in countercurrent flow to the sand. Here, the steam flows successively through the superheater, evaporator and finally through the economizer. The substantial advantages of this technology over the technology of the FBC are, that there are no large energy requirements for operation, no additional units (e.g. for fluidization) are required and several functions of the steam generator (preheating, evaporation, overheating) can be covered with one apparatus. Due to external heat transfer coefficient from sand to steam generator tubes is by MBHX lower as by FBC, the apparatus becomes specifically larger.

For calculating the heat transfer from the bulk to the water-steam cycle, the two heat transfer coefficients for the inside and outside are required. The outer heat transfer coefficient consists of the heat transfer between the wall and the particles and heat transfer through the bed. The calculation algorithm is shown by Schlünder [15]. The internal heat transfer coefficients of the sections economizer, evaporator and superheater are calculated using different correlations. So, for economizer and superheater Nusselt equations from the VDI Heat Atlas [4] are used; and for the evaporator an equation for the calculation of the heat transfer coefficient from Strauss [16] is chosen, that is only valid in case of evaporation and condensation processes. The calculation of the pressure loss is based on VDI Heat Atlas [4].

Water-Steam Cycle

The water-steam cycle is operated with a fixed pressure, i.e. the live steam pressure does not change even in partial load operation. This operation mode has the advantage of rapid power dynamic [16]. For the simulation 540 °C and 100 bar are assumed as the live steam parameters. The condensing pressure is set to 0.1 bar.

The nominal electrical output of the generator is 50 MW. The thermal power required for this is supplied mainly from the sand mass flow. In addition, the fluidization air must be heated to bed temperature and heat losses to the environment are considered.

An optional regenerative feed water heating is considered to increase the efficiency of the water-steam cycle. This measure has to be compared with the advantage of a lower sand outlet temperature.

PARAMETRIC STUDY

Following parameters were examined in the parametric study: The number of FBC, grain diameter of the sand, cold sand temperature, size of the ASHX, steam parameters, application of regenerative feed water heating. The results were used to dimension the individual components, to determine the optimum operating parameters and were finally used as the default values for the system simulation of annual performance calculations.

All parameter variations have been done with the irradiation data of the reference day (March 21) at the location of Huelva (Spain) with design point of the system and its components at Solar Noon (time of highest irradiation, see Fig. 3 (b)) while getting a solar multiple of two. This means that exactly half of the thermal input at the receiver is stored, while the other half will be used directly for electricity production. At other times of the reference day the calculation is performed in part load mode and the electricity yield throughout the day is determined. The irradiation data of the reference day are idealized and are not real weather data. In contrast, for annual performance calculations weather data for year 2005 from Huelva are used.

Grain Diameter of the Sand

The grain diameter of the sand is one of the main factors influencing the yield of the power plant, as it affects the heat transfer and pressure drop in the ASHX and FBC or MBHX. The heat transfer in the fluidized beds is significantly high [10] when particle size is less than 1 mm. Thus, the required heat transfer area, and whereby the electrical energy demand for fluidization decreases. In ASHX reduced grain size also leads to better heat transfer coefficient, but to the increased pressure loss too. Therefore, to get the economic optimum of the system the positive and negative impacts of grain diameter size have to be assessed.

Figure 3 (a) shows the simulation results of a particle size variation. The generated net electricity is plotted as a function of the grain diameter of the sand. The optimum grain diameter for this system configuration is at about 0.8 mm. In the model with MBHX the optimal diameter is significantly higher at about 2.1 mm. For smaller particle sizes (< 0.8 mm) the electricity yield is dominated by the power demand of the fan. For larger particle sizes (> 0.8 mm) the energy demand needed for fluidization outweighs. The course of the net electrical power throughout the day illustrates this situation (see Fig. 3 (b)). As can be clearly seen, the net output of the power plant decreases significantly at noon when the sun is at its highest point. During this period the highest air mass flow is required, resulting in a disproportionate increase in motor power of the fan. Due to the increased pressure loss in the ASHX with smaller grain sizes, this drop in power output enhanced with decreasing grain diameter.

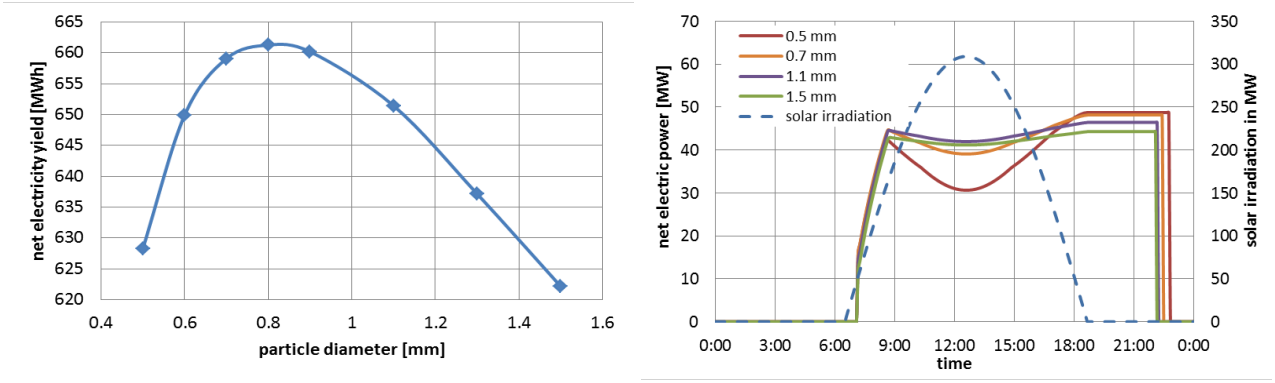

(a) (b)

FIGURE 3. Net electricity yield at reference day vs. grain sizes of the sand (a), Net electricity power and idealized solar irradiation vs. reference day time (b)

Cold Sand Temperature

The cold sand temperature is another important factor influencing the profitability of the power plant. In principle, it is desirable to achieve the lowest possible temperature, because the rise in temperature difference at the heat exchangers results in lower mass flow of sand and air. This returns a lower fan power demand, as can be seen in Fig. 4 (a), where the fan power at the maximal irradiation at the receiver of 410 MW in the year 2005 is drawn for different cold sand temperatures and grain sizes. It is obvious, that the fan power demand decreases with decreasing cold sand temperature. What cold sand temperature could be reached depends on the design of the FBC. The lower the cold sand temperature, the greater the required heat transfer area, which reflected in the energy consumption of the FBC.

Figure 4 (b) shows the net electricity yield of the power plant at the reference day depending on the cold sand temperature at different grain sizes. For smaller particle diameters, the optimum cold sand temperature moves towards lower values. The global optimum is at a grain size of about 0.8 mm and a cold sand temperature of 260 °C with and of 240 °C without regenerative feed water heating consequently. However, the maximum electricity yield varies only slightly by a few MWh depending on the grain size. Significant impact, however, has the regenerative feed water heating: The net electricity yield is about 37 MWh higher compared to system without regenerative feed water heating, which corresponds to system efficiency increase of 5.6 %.

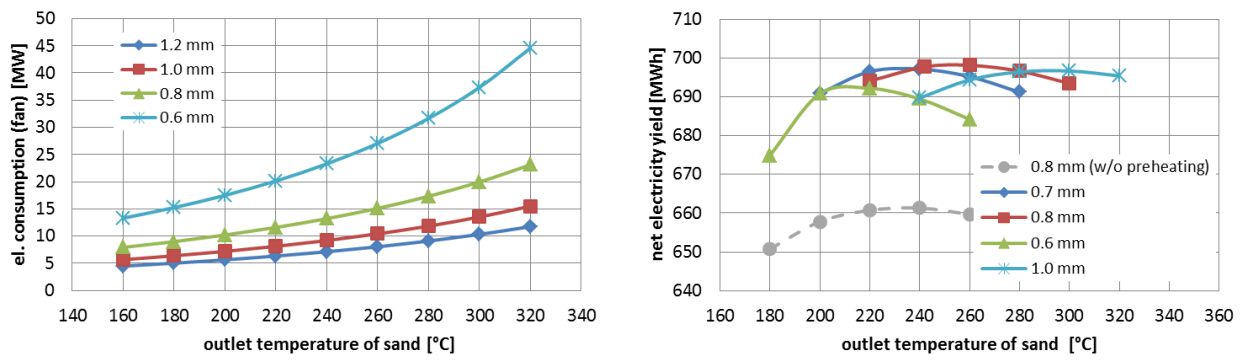

(a) (b)

FIGURE 4. Fan power vs. cold sand temperature at different grain size at maximal irradiation (a), Net electricity yield vs. cold sand temperature at different grain size with or without regenerative feed water heating (b)

Optimal Operating Parameters

First, the dimensions of the ASHX are set: flow-through length of the apparatus is 0.05 m and the cross-sectional area is 600 m². The optimal values of the operating parameters listed in Table 1 are resulted from the performed parametric study.

TABLE 1. Overview of optimal operating parameters.

Description	Value	Unit	Source
Number of FBC	6 (1 x SUPHTR, 2 x EVAP, 3 x ECO)		Design value
Grain diameter	0.8	mm	Simulation result
Air inlet temperature at ASHX	850	°C	Design value
Sand outlet temperature at ASHX	800	°C	Design value
Air outlet temperature at ASHX	variabel	°C	
Sand inlet temperature at ASHX (without regenerative feed water heating)	240	°C	Simulation result
Sand inlet temperature at ASHX (with regenerative feed water heating)	260	°C	Simulation result
Live steam temperature	560	°C	Design value
Live steam pressure	100	bar	Design value
Bed length ASHX	0.05	m	Design value
Cross-sectional area ASHX	600	m²	Design value

SYSTEM SIMULATION AT OPTIMAL PARAMETERS

Annual performance calculations are performed based on real weather data form 2005 at Huelva (Spain). Finally, a comparison between the two system models with FBC or MBHX is be made.

Annual Performance Calculations

The storage size is fixed at 12,000 t. At extreme days, it may happen that the storage reaches its full capacity. In this case, the irradiation on the receiver is reduced so much that no additional sand is stored and the power plant can be operated at nominal power (defocusing).

During the annual performance calculations it is analyzed, which proportion on total electricity yield of the power plant is caused by the sand storage system and how would be the yield without storage. For this evaluation, the amount of the hot sand stored over the year is summarized. In addition, it is calculated how much more electricity demand for the fan and the FBC is needed while using the storage system. The results of the annual performance calculations with and without regenerative feed water heating are presented in Table 2.

TABLE 2. Results of the annual performance calculations and influence the storage operation.

Description	Unit	Without regenerative feed water heating	With regenerative feed water heating
Net electricity yield	GWh_{el}	223.1	234.2
Gross electricity yield	GWh_{el}	251.5	265.9
Amount of internal energy demand	%	11.3	11.9
Demand for pump power	GWh_{el}	3.7	4.0
Stored sand mass	$10^6 \cdot t$	1.55	1.73
Electrical yield from storage	GWh_{el}	92.5	111.9
Overall energy consumption of fan	GWh_{el}	16.5	18.7
Additional energy consumption of fan (storage)	GWh_{el}	8.1	9.8
Thermal losses of storage	GWh_{el}	0.9	1.2
Overall energy consumption FBC	GWh_{el}	8.3	8.5
Additional energy consumption FBC (storage)	GWh_{el}	2.7	3.0
Utilization rate	%	27.7	29.1
Net electrical yield without storage	GWh_{el}	142.3	136.2
Utilization rate without storage	%	17.7	16.9

Approximately half of the energy demand of the fan is caused by charging hot sand and 30 % more energy is required for the FBC, because of more operating hours. This proportion become void if storage is not used and the energy input by sun is limited. Regarding the net electricity yield, 41 % comes from storage system in the power plant without and 48 % in the power plant with regenerative feed water heating. Despite higher energy consumption for fan and FBC, the electricity yield is more than a third greater with storage usage.

The energy requirement of the power plant is about 12% of which approximately 60 % accounts on the fan and around 27-29 % on the FBC.

Taking into account losses in the collector field with 60 %, results in an overall efficiency of the plant by 16.6 % and 17.5 %. The values are slightly higher than the data of Viebahn et al. [17] where an utilization rate of about 15 % is published.

The storage capacity used for simulation is limited at 12,000 t. Upon reaching full capacity, the thermal input is reduced, so that no further hot sand more is stored. The number of days on which this condition occurs is dependent on the dimensioning of storage. Table 3 shows the number of days the storage is fully loaded and how much solar radiation thus remains unused.

In the plant with regenerative feed water heating the storage comes more often to its limits. The reason is the increased cold sand temperature compared to the system without regenerative feed water heating. The sand mass flow in the ASHX is at about 17 kg/s larger at design point and even more hot sand can be stored.

In total, the power plant will be 5260 h or 5520 hours per year in operation and the storage system participate in 2313 h or 2547 h. 1616 h or 1859 h account for the time after sunset, so that the power plant is operated average 4.4 h or 5.1 h after sunset.

TABLE 3. Overview defocusing by reaching the storage capacity limit.

Regenerative feed water heating	Days with defocusing	Total time of defocusing	Unused irradiation	Proportion of total irradiation
	D	h	MWh_{th}	%
Without	4	3.75	374	0.05
With	21	35.75	4158	0.52

System Comparison FBC vs. MBHX

For technology comparison reasons, additional to the system with fluidized bed cooler (FBC) an identical power plant with moving bed heat exchanger (MBHX) is simulated. The target is to evaluate the impact of the use of different technologies for generating steam on the net electricity yield of the power plant and on the size of the steam generator.

Although the calculated heat transfer coefficient at the outside of the tubes in the FBC is 2-2.5 times higher than in MBHX, the volume of the apparatus is only 25 % smaller for technological reasons. Summarizing it can be said that the use of FBC in the considered system provides only slight advantages in terms of size compared to the MBHX. Disadvantages are further investments associated with the FBC - such as compressors and heat exchangers to provide the fluidization air. As seen in Table 4, the net electricity yield is 6.2 % lower when using a FBC instead of a MBHX. The energy requirements of the fan are significantly higher, due to the smaller particle size, but are compensated partly by the increased gross electricity yield, caused by additional heat input of the fan. Thus, in the present configuration the system with MBHX is preferable that with FBC.

TABLE 4. Comparison between model with MBHX and model with FBC (system with regenerative feed water heating).

	W_{GROSS}	W_{NET}	$W_{AUX,total}$	W_{fan}	W_{FBC}
	GWh_{el}	GWh_{el}	GWh_{el}	GWh_{el}	GWh_{el}
MBHX	258.56	249.74	8.82	4.05	-
FBC	265.9	234.2	31	18.7	8.5

RESULTS AND CONCLUSIONS

The parametric studies give valuables insights into the systems behavior: It elaborates the determining factors the systems performance, such as grain diameter and cold sand temperature. Also, the results indicate that the net electricity production of the power plant is mainly influenced by the two main electric consumers, namely the fans to fluidize the fluidized bed cooler and the fan of the air cycle.

The use of MBHX for steam generation is turned out advantageous compared to FBC. The former is a little bit more compact, but has a substantially higher parasitical energy demand.

The use of granular bulk material as a heat storage medium in solar thermal power plants is a promising alternative to the conventional liquid salt storage systems. Technical hurdles associated with this alternative are demanding, but can be resolved. From a preliminary assessment it is expected that this new concept can result in a substantial cost reduction compared to state-of-the-art CSP technology.

ACKNOWLEDGMENTS

The authors would like to thank the German Federal Ministry for Economic Affairs and Energy for financial support of the HiTExStorII-project.

REFERENCES

1. S. Warerkar et al., J SOL ENERG-T ASME **133 (2)**, pp. 021010-1–7 (2011).
2. S. Warerkar et al., Verfahrenstechnik, no. 4, pp. 72–73 (2007).
3. E. Achenbach, EXP THERM FLUID SCI **10 (1)**, pp. 17–27 (1995).
4. Verein Deutscher Ingenieure, *VDI Heat Atlas* (Springer, Berlin, Heidelberg, 2011).

5. N.N., “Technische Chemie II - Filtration, Vorlesung,“ Universität des Saarlandes, Saarbrücken, 2004.
6. B. Spang and W. Roetzel, HEAT MASS TRANSFER **30**, pp. 417–422 (1995).
7. K.-E. Wirth, *Zirkulierende Wirbelschichten*, (Springer, Berlin, Heidelberg, 1990).
8. A. Mersmann, CHEM-ING-TECH **39**, pp. 349–353 (1967).
9. H. Martin, CHEM-ING-TECH **52 (3)**, pp. 199-209, 1980.
10. E.-U. Schlünder and E. Tsotsas, “Wärmeübergang zwischen Gas-Feststoff-Wirbelschichten und den Oberflächen eingebauter Heizelemente“ in *Wärmeübertragung in Festbetten, durchmischten Schüttgütern und Wirbelschichten* (Thieme, Stuttgart, New York, 1988), pp. 216-231.
11. D. Kunii und O. Levenspiel, “Heat Transfer between Fluidized Beds and Surfaces“ in *Fluidization Engineering*, (Butterworth-Heinemann, Boston, 1991), pp. 313-335.
12. H. Effenberger, *Dampferzeugung*, (Springer, Berlin, Heidelberg, 2000.)
13. T. Baumann and S. Zunft, J. Phys.: Conf. Ser. **395** 012055 (2012).
14. T. Baumann, S. Zunft and R. Tamme, HEAT TRANSFER ENG **35** (3), pp. 224-231 (2014).
15. E. U. Schlünder, CHEM ENG PROCESS **18** (1), pp. 31-53 (1984).
16. K. Strauß, *Kraftwerkstechnik*, (Springer, Heidelberg, 2009).
17. P. Viebahn, Y. Lechon and F. Trieb, Energy Policy **39 (**8), pp. 4420-4430 (2011).